Boundary Element Method: Final Report

Travis Simpson
MATH3001

July 4, 2022

Contents

Chapter 1

Introduction

The Boundary Element Method (BEM) is a numerical method that solves partial differential equations inside a domain by expressing them as *boundary integral equations*. This report studies the conceptualisation and formulation of the BEM, primarily with focus upon the *Laplace equation* within the domain. Starting from the fundamental solution of the Laplace equation in two and three dimensions, we use Green's Second Identity to express the function T inside the boundary in terms of a *boundary integral equation*. Then we discretise this equation into so-called *boundary elements* and evaluate them at their midpoints to complete the final step of deriving the BEM.

Beyond this we will briefly look at some other partial differential equations inside the domain and formulate them into problems involving the Laplace equation or into boundary integral equations. Finally, we will solve some basic problems (Dirichlet and Robin type) by coding the BEM in Python, which will allow us to show that the method works best for a larger number of (smaller) boundary elements. Furthermore we will see that the method is equally effective at evaluating points near to and far from the boundary when we calculate the relative error, and also that the method converges *quadratically* to the exact value as we increase the number of elements N.

Before beginning, it is worth briefly considering not only the purpose of this research, but also the value of it as academic work. The objective of this report is to provide a source on the BEM that is clear to understand for almost any undergraduate studying mathematics, and also hopefully accessible to students in other STEM fields such as engineering - an area where the applications of the research are particularly pertinent. There are many uses for the BEM, ranging from elastostatics to fracture mechanics (see chapters 2 & 8 by Aliabadi, 2002), and we will briefly cover heat transfer and fluid dynamics. Thus it is hard to see how this research could be in any way morally contentious, and hopefully instead it could prove to be a useful starting point for anyone who wants to delve deeper into this particular discipline.

1.1 Literature Review

The Boundary Element Method owes its discovery to many mathematicians over the past three centuries. As is always the case with mathematics, new findings are formed from previously proven theories and the BEM is no exception to this rule. In fact, it is one of the best examples of this behaviour due to the highly collaborative nature of its discovery. As Cheng, A. & Cheng, D. (2005) point out, the BEM was born from a "series of connected efforts" (p.269) that led to a movement in the late 1960s. This means that this boundary method is not only rich with historical significance from mathematical findings as early as those from Euler in the 18^{th} century, but also rife with international cooperation from when it was developed in the second half of the 20^{th} century. All of this means that there was no 'eureka moment' in which the method was discovered, but a slow process beginning with integral theorems and equations, truly taking off once numerical methods were able to be done computationally. Both *'Heritage and early history of the boundary element method'* by Cheng, A. & Cheng, D. (2005) and *'The birth of the boundary element method from conception to application'* by Brebbia, C. (2017) look at the processes and history of the BEM but take slightly different approaches. This section aims to analyse and compare the two articles and to see what (if anything) could be done to improve or build upon their work.

Cheng, A. & Cheng, D. investigate the very early history of the method and build upon theories and equations leading up to the late 1970s, where journal articles about the BEM began to grow significantly. They begin, however, by comparing the BEM with the Finite Element Method (hereafter FEM) and the Finite Difference Method (hereafter FDM), or so-called domain methods, noting that the reduction in dimension from the BEM creates easier systems for a computer to deal with, both more quickly and requiring less computer memory. The BEM is also more suitable to (i.e. is designed to) model at unbounded domains than the domain methods, which would have to truncate the domain and therefore approximate their solutions.

In line with the comparisons of the methods, the authors analyse the prevalence of the three methods by the number of journal article publications on each respective method. This inspection leads to the result that the domain methods FEM and FDM appear more frequently in publications than the BEM. However, there are caveats to the approach they take. In order to compare the amount of publications, they searched for key phrases relating to the methods, but the search only looks through the titles, keywords, and abstracts of the articles it looks at. They acknowledge that not all articles contain abstracts and keywords, leaving only the title to contain the matching phrase (p.298). This means that many pertinent articles could have been missed out, so although the data they collected could still be considered reliable, or at the very least indicative, one must acknowledge (as they themselves state) that there are potential flaws with their

methodology.

Brebbia (2017) does not compare the methods quantitatively. Although the FDM does not get mentioned at all in his article, the FEM is compared with the BEM on their differences and indeed similarities in technique (e.g. the reduction of dimension in the BEM (p.7)). The author also opines that the FEM and BEM should be recognised as complementary to one another rather than in some form of competition (p.9). This school of thought is understandable given Brebbia's successful work on both the FEM and BEM (Cheng, A. & Cheng, D., 2005, p.297). The other article implies that there is some competitive aspect to the different types of methods by comparing figures and their respective prevalence in the academic realm. Any subject areas that are considered to be in tandem with one another would not likely be compared with each other in the way that the authors decided to do, but instead would be looked at together in the same set of figures (i.e. the total sum of all three methods' publications). The authors also look at the number of journal articles about the BEM published from 1974 until 2003 and demonstrate nicely the rapid (seemingly exponential) growth of interest in the subject from the seventies to the early nineties. We can see that this has now plateaued out and the number of publications on the BEM is roughly 700-800 each year. They compare this to 5000 and 1400 articles per year for the FEM and FDM respectively, further putting the methods at odds with each other (p.269).

Looking at the mathematics/equations they both include in their articles, we see that both sets of work begin by looking at the widely applicable Laplace equation $\nabla^2 u = 0$. Cheng, A. & Cheng, D. decide to incorporate more basic equations from vector calculus and fluid mechanics, introducing and applying concepts such as divergence and curl as well as incompressible and irrotational fluid flows (p.270). Brebbia on the other hand assumes a greater understanding from his readership and enters almost directly into applied integral equations of BEM systems (p.5).

They also both acknowledge the pioneering work of George Green, whose identities, functions, and formula are pivotal to many branches of modern mathematics. Cheng, A. & Cheng, D. list Green's identities along with the Divergence Theorem $\iiint_V \nabla \cdot \mathbf{F}\, dV = \oiint_S \mathbf{F} \cdot d\mathbf{S}$, which also plays a major role in the BEM as it turns a volume integral into a surface integral, thus reducing the dimensionality of the problem by one. They also include other important integral theorems of vector calculus, such as Stokes's Theorem among others. Since these are relevant to the BEM, they are worth including in an historical overview of the boundary method. Brebbia however not only assumes a greater base knowledge of the reader, but also does not decide to go into too much detail about anything outside of the 1970s to the 1980s, so sees no need for an in-depth description of the complete fundamentals of the mathematical basis upon which the domain and bound-

ary methods were developed. With Brebbia being such a core figure of the development of the BEM in this time period, it is understandable for him to focus on these decades so that he provides readers with a first-hand account of his experiences.

Since it is a longer article, *'Heritage and early history of the boundary element method'* is able to include short personal biographies of the mathematicians (including Brebbia) who were pivotal to the BEM's development. Although this is not an absolutely essential addition to the history of the BEM, it adds an extra dimension (unlike the BEM) to just their mathematical discoveries alone. We see not only their achievements, but also the struggles that they experienced and the perseverance they displayed in order to overcome all challenges that emerged.

Due to the nature of Brebbia's article, he looks at more applied cases of the BEM. He uses illustrations alongside explanations to give the reader an understanding of what the BEM can be used for and to show the reader its place in the modern world. He looks at problems which have an infinite domain, meaning that the BEM is a good candidate to find a solution. For example, he considers offshore rigs, onshore foundations, and electromagnetic radiation affecting the human body (p.8). With this, he opens up not only the history of the discovery of the BEM, but also the current everyday applications that can be and are being used to solve/prevent issues.

Overall, both texts approach the topic slightly differently to each other. Brebbia employs a more practical and modern approach that is rife with examples related to engineering. He only briefly discusses mathematicians from the 19^{th} century in his introduction and dedicates the rest of the article to write about the time period in which he was involved. This provides a unique perspective into the developments that occurred during the inception of the BEM in the 1970s and 80s. Unlike Brebbia's work, Cheng, A. & Cheng, D. do look at mathematicians and their discoveries over the last three centuries and chronologically guide the reader through the stages that led up to the BEM's birth all the way from Euler in the 18^{th} century. They include plenty of integral and differential equations that build upon each other to arrive at the BEM. Their article could benefit from more visual applications of the BEM as seen in Brebbia's work, as this would provide an insight into the role of the boundary method in the modern age. Also, their comparison of domain method publications versus boundary method publications could be seen as pitting the two methods against each other, which as Brebbia concludes could be counterproductive.

Chapter 2

Boundary Element Method for Laplace's Equation

In this chapter, we will derive the procedure of the boundary element method for Laplace's equation $\nabla^2 T = 0$ inside the domain by taking the following steps:

1. Derive a fundamental solution of the underlying differential operator defining the problem (in this case, the *Laplacian* ∇^2).

2. Use this fundamental solution (if it exists) and Green's identities to transform the governing PDE into a boundary integral equation (BIE).

3. Discretise the boundary into small (linear or nonlinear) *boundary elements*. Since these boundary elements will become very small, the unknown functions and their normal derivatives (e.g. temperature T & flux $\frac{\partial T}{\partial n}$) can be approximated by constants. Now, the BIE can be discretised and include the same approximations.

4. Apply the discretised equation at the nodes (i.e. midpoints in 2D) in each element. Then we get a system of linear algebraic equations, which are completed by imposing the boundary conditions.

5. The solution of the system of equations produces the remaining boundary data. Values of the unknown function inside the domain can then be determined numerically.

The task of meshing a boundary in 3D comes with many of its own topological theorems, which will not be covered in detail here (see instead chapter 14 by Maor, 1987). Briefly, there are three polygons which can tile a plane by themselves without leaving any gaps, namely equilateral triangles, squares, and hexagons, the latter of which are merely a variation of the former (Maor, 1987, p.102). There are of course other irregular or nonuniform shapes and combinations that are possible in a mesh, but these could

impede the processing speed of the computation and vastly increase the complexity of the program, so the boundary element method typically uses quadrilateral or triangular elements (Brebbia & Walker, 1980, p.65). Here, we will mostly focus on the 2D case with linear boundary elements, particularly in specific examples. We could also consider the fact that more elements are required when modelling sharp curves, and fewer elements are necessary to model straight edges on the domain (see Figure 2.3 demonstrating why this is the case).

2.1 The Fundamental Solution to the Laplace Equation

It is important for researchers to be able to determine when the BEM is a suitable choice of method (and when it is not). For example, not all PDEs can be expressed as an integral equation, so in these instances we cannot use the BEM independently (Yu, 2010, p.885). If the fundamental solution of the differential operator cannot be found (for example, if the coefficients of the differential operator are not constant), then it is possible to implement a coupling of the FEM and BEM by splitting the domain Ω such that one part Ω_1 contains the inhomogeneities, and the other subdomain Ω_2 is described by a differential operator with constant coefficients which can be solved (Costabel, 1987, pp.268-9). We will look at problems where the Laplace equation governs the behaviour inside the bounded domain, and so a fundamental solution can be found.

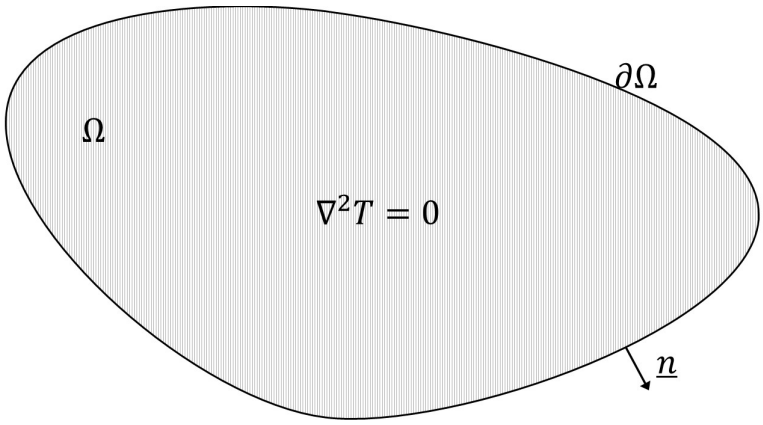

Figure 2.1: The bounded domain Ω where $\nabla^2 T(\underline{p}) = 0$ for $\underline{p} \in \Omega$ (i.e. T is harmonic).

The fundamental solution to the Laplacian is found by solving the generalised function satisfying $\nabla^2_{\underline{p}'} G(\underline{p}, \underline{p}') = -\delta(\underline{p} - \underline{p}')$ where $\underline{p} \in \Omega$, $\underline{p}' \in \partial\Omega$, and $\delta(\underline{p} - \underline{p}')$ is the *Dirac Delta function.*

2.1.1 The Two-Dimensional Case

We begin in 2D by solving the general solution to $\nabla^2_{\underline{p}'} G = 0$ for $\underline{p} \neq \underline{p}'$ where $G(\underline{p}, \underline{p}') = G(r)$ is a so-called radial function (Sharp, 2021, p.50), meaning it only depends on the radius $r = |\underline{p} - \underline{p}'| = \left((x-x')^2 + (y-y')^2\right)^{1/2}$. This allows Laplace's equation (a PDE) to be reduced to an ODE, so

$$\begin{aligned} 0 = \nabla^2 G(r) &= \left(\frac{\partial^2}{\partial x^2} + \frac{\partial^2}{\partial y^2}\right) G(r) = \frac{\partial}{\partial x}\left(\frac{\partial G}{\partial r}\frac{\partial r}{\partial x}\right) + \frac{\partial}{\partial y}\left(\frac{\partial G}{\partial r}\frac{\partial r}{\partial y}\right) \\ &= \frac{\partial^2 G}{\partial r^2}\left(\frac{\partial r}{\partial x}\right)^2 + \frac{\partial G}{\partial r}\frac{\partial^2 r}{\partial x^2} + \frac{\partial^2 G}{\partial r^2}\left(\frac{\partial r}{\partial y}\right)^2 + \frac{\partial G}{\partial r}\frac{\partial^2 r}{\partial y^2} \\ &= \frac{\partial^2 G}{\partial r^2}\left(\left(\frac{\partial r}{\partial x}\right)^2 + \left(\frac{\partial r}{\partial y}\right)^2\right) + \frac{\partial G}{\partial r}\left(\frac{\partial^2 r}{\partial x^2} + \frac{\partial^2 r}{\partial y^2}\right). \end{aligned} \tag{2.1}$$

But $\frac{\partial r}{\partial x} = r_x = \frac{1}{2}2(x-x')\left((x-x')^2 + (y-y')^2\right)^{-1/2} = \frac{x-x'}{r}$ and equivalently $r_y = \frac{y-y'}{r}$. Then $r_{xx} = \frac{(y-y')^2}{r^3}$ & $r_{yy} = \frac{(x-x')^2}{r^3}$. Putting these into equation (2.1) gives the Laplace equation in polar coordinates

$$\begin{aligned} \nabla^2 G(r) &= \frac{\partial^2 G}{\partial r^2}\left(\frac{(x-x')^2 + (y-y')^2}{r^2}\right) + \frac{\partial G}{\partial r}\left(\frac{(x-x')^2 + (y-y')^2}{r^3}\right) \\ &= \frac{\partial^2 G}{\partial r^2} + \frac{1}{r}\frac{\partial G}{\partial r} = \frac{1}{r}\frac{\partial}{\partial r}\left(r\frac{\partial G}{\partial r}\right) = 0. \end{aligned}$$

Integrating once gives

$$r\frac{\partial G}{\partial r} = c_1$$

and rearranging and integrating again gives the general solution

$$G(r) = c_1 \ln(r) + c_2$$

where $c_1, c_2 \in \mathbb{R}$ are real constants. We set $c_2 = 0$ arbitrarily and to find c_1, we must look at the magnitude when $\underline{p} = \underline{p}'$. So integrate $\nabla^2_{\underline{p}'} G(\underline{p}, \underline{p}') = -\delta(\underline{p} - \underline{p}')$ over the circle B_ϵ with radius $\epsilon > 0$ and centred at $\underline{p} = \underline{p}'$ to get

$$-\int_{B_\epsilon} \nabla \cdot \nabla G(\underline{p}, \underline{p}')\, dB_{\underline{p}} = \int_{B_\epsilon} \delta(\underline{p} - \underline{p}')\, dB_{\underline{p}} = 1,$$

where we have used the property of the *Dirac Delta function*. Applying the *Divergence Theorem*, we get

$$-\int_{S_\epsilon} \underline{n} \cdot \nabla G(\underline{p}, \underline{p}')\, dS_{\underline{p}} = -\int_{S_\epsilon} \frac{\partial G(\underline{p}, \underline{p}')}{\partial n}\, dS_{\underline{p}}$$

$$= -\int_{S_\epsilon} \frac{\partial G(r)}{\partial r}\, dS_{\underline{p}} = 1, \tag{2.2}$$

where $S_\epsilon = \partial B_\epsilon$ and $dS_{\underline{p}} = r\, d\phi$ for $0 \leq \phi \leq 2\pi$ (Kythe, 1996, p.79). We have $G(r) = c_1 \ln r$, so $\frac{\partial G}{\partial r} = \frac{c_1}{r}$ in equation (2.2) gives

$$1 = -\int_0^{2\pi} \frac{c_1}{r} r\, d\phi = -c_1 \int_0^{2\pi} d\phi = -2\pi c_1 \quad \Rightarrow\ c_1 = -\frac{1}{2\pi}.$$

So the fundamental solution for the Laplace equation in two-dimensional space is

$$G(r) = -\frac{1}{2\pi} \ln(r). \tag{2.3}$$

2.1.2 The Three-Dimensional Case

Now looking at the 3D case, we put the Laplace equation $\nabla^2_{\underline{p}'} G = 0$ in radial-spherical coordinates to get

$$\frac{1}{r}\frac{d}{dr}\left(r^2 \frac{dG}{dr}\right) = 0.$$

Solving gets $G(r) = \frac{c_3}{r} + c_4$, so we take $c_4 = 0$ and solve for c_3 in equation (2.2) with $dS_{\underline{p}} = r^2 \sin(\theta)\, d\theta\, d\phi$ and $0 \leq \theta \leq \pi$, $0 \leq \phi \leq 2\pi$. Now $\frac{dG}{dr} = -\frac{c_3}{r^2}$, so we get

$$1 = \int_0^{2\pi}\int_0^{\pi} \frac{c_3}{r^2} r^2 \sin\theta\, d\theta\, d\phi = \int_0^{2\pi} d\phi \int_0^{\pi} c_3 \sin\theta\, d\theta = 2\pi c_3 \left[-\cos\theta\right]_0^{\pi} = 4\pi c_3$$

$$\Rightarrow c_3 = \frac{1}{4\pi}.$$

So the fundamental solution for the Laplace equation in three-dimensional space is

$$G(r) = \frac{1}{4\pi r}. \tag{2.4}$$

2.2 Boundary Integral Equations

We use Green's Second Identity to derive a formula for $T(\underline{p})$. For all functions ϕ and ψ,

$$\int_\Omega (\phi \nabla^2 \psi - \psi \nabla^2 \phi)\, d\Omega = \int_{\partial\Omega} \left(\phi \frac{\partial \psi}{\partial n} - \psi \frac{\partial \phi}{\partial n}\right) dS.$$

Now let $\phi = T$ and note $\nabla^2 T = 0$. Also let $\psi = G$ (i.e. the fundamental solution) and recall $\nabla^2_{\underline{p}'} G(\underline{p}, \underline{p}') = -\delta(\underline{p} - \underline{p}')$. Thus, we can use the properties of the *Dirac Delta function* to show

$$T(\underline{p}) = \int_{\partial\Omega} \left(G(\underline{p}, \underline{p}') \frac{\partial T}{\partial n}(\underline{p}') - T(\underline{p}') \frac{\partial G}{\partial n}(\underline{p}, \underline{p}')\right) dS \tag{2.5}$$

for $\underline{p} \in \Omega$ not on the boundary.

But what if $\underline{p}$ lies on the boundary? We are trying to bind $\underline{p}$ to the boundary $\partial\Omega$, so we integrate over a hemisphere $B_\epsilon \subset \Omega$ of radius ϵ centred at the boundary point $\underline{p}' \in \partial\Omega$ where $\underline{p} \in B_\epsilon$ as the hemisphere shrinks to the boundary (i.e. $\epsilon \to 0$).

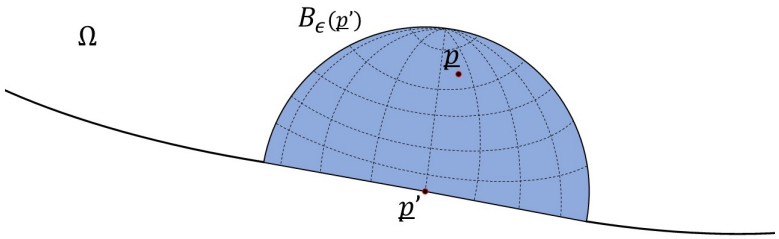

Figure 2.2: Hemisphere $B_\epsilon(\underline{p}') \subset \Omega$ shrinking to the boundary with $\underline{p} \in B_\epsilon(\underline{p}')$ & $\underline{p}' \in \partial\Omega$.

Starting in 3D with the first integral term of equation (2.5) and using equation (2.4) which defines $G(\underline{p}, \underline{p}')$, followed by the standard formula for the surface area of a hemisphere $S = 2\pi r^2$, we get via Partridge *et al* (1991, pp.16-18)

$$\lim_{\epsilon\to 0}\left(\int_{B_\epsilon} G\frac{\partial T}{\partial n}\,d\Omega\right) = \lim_{\epsilon\to 0}\left(\int_{B_\epsilon} \frac{1}{4\pi\epsilon}\frac{\partial T}{\partial n}\,d\Omega\right) = \lim_{\epsilon\to 0}\left(\frac{2\pi\epsilon^2}{4\pi\epsilon}\frac{\partial T}{\partial n}\right) = 0,$$

or for 2D using equation (2.3) where the semicircle perimeter is $\pi\epsilon$

$$\lim_{\epsilon\to 0}\left(\int_{B_\epsilon} G\frac{\partial T}{\partial n}\,d\Omega\right) = \lim_{\epsilon\to 0}\left(-\frac{\pi\epsilon\ln\epsilon}{2\pi}\frac{\partial T}{\partial n}\right) = 0.$$

Now for the second integral term of equation (2.5) in 3D, we know from equation (2.4) that $G(\epsilon) = \frac{1}{4\pi\epsilon}$, so $G'(\epsilon) = -\frac{1}{4\pi\epsilon^2}$. Using this with the surface area of the hemisphere again, we find

$$\lim_{\epsilon\to 0}\left(-\int_{B_\epsilon} T\frac{\partial G}{\partial n}\,d\Omega\right) = \lim_{\epsilon\to 0}\left(\int_{B_\epsilon} T\frac{1}{4\pi\epsilon^2}\,d\Omega\right) = \lim_{\epsilon\to 0}\left(T\frac{2\pi\epsilon^2}{4\pi\epsilon^2}\right) = \frac{1}{2}T,$$

or for 2D using equation (2.3) where $G'(\epsilon) = -\frac{1}{2\pi\epsilon}$ and semicircle perimeter $\pi\epsilon$

$$\lim_{\epsilon\to 0}\left(-\int_{B_\epsilon} T\frac{\partial G}{\partial n}\,d\Omega\right) = \lim_{\epsilon\to 0}\left(T\frac{\pi\epsilon}{2\pi\epsilon}\right) = \frac{1}{2}T.$$

So for the boundary point $\underline{p} \in \partial\Omega$, we have found

$$\int_{\partial\Omega} \left[G(\underline{p}, \underline{p}') \frac{\partial T}{\partial n}(\underline{p}') - T(\underline{p}') \frac{\partial G}{\partial n}(\underline{p}, \underline{p}') \right] dS = \frac{1}{2} T(\underline{p}). \tag{2.6}$$

2.3 Numerical Discretisation of the Boundary

Now we discretise the boundary $\partial\Omega$ into linear *boundary elements* Γ_j with endpoints $\underline{p}_{j-1}$ & $\underline{p}_j$ for $j = 1, \ldots, N$. Over each Γ_j, we assume T and its normal derivative $\frac{\partial T}{\partial n}$ to be constants, taking their values at the midpoint node $\underline{\tilde{p}}_j$ of the boundary element. Thus $T(\underline{p}) = T(\underline{\tilde{p}}_j) =: T_j$ and $\frac{\partial T}{\partial n}(\underline{p}) = \frac{\partial T}{\partial n}(\underline{\tilde{p}}_j) =: T'_j$ where $\underline{p} \in \Gamma_j$.

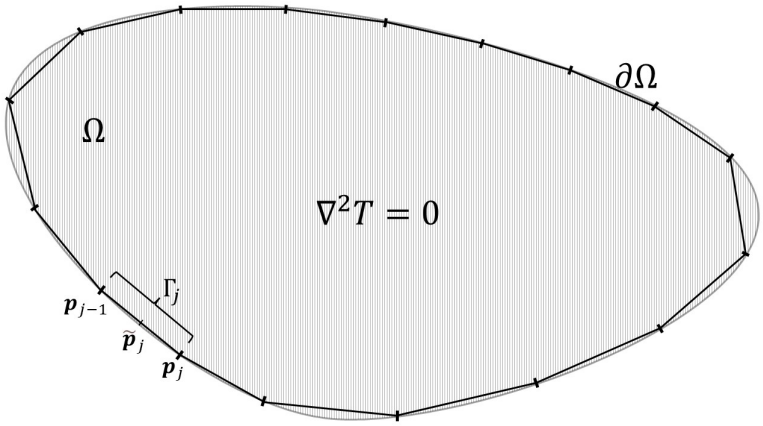

Figure 2.3: Discretisation of boundary $\partial\Omega$ into boundary elements Γ_j with midpoint $\underline{\tilde{p}}_j$.

So over each boundary element, we can rewrite equation (2.6) as

$$\eta(\underline{p}) T(\underline{p}) = \sum_{j=1}^{N} \left[T'_j \int_{\Gamma_j} G(\underline{p}, \underline{p}') \, d\Gamma_j - T_j \int_{\Gamma_j} \frac{\partial G(\underline{p}, \underline{p}')}{\partial n} \, d\Gamma_j \right]. \tag{2.7}$$

Let

$$A_j = \int_{\Gamma_j} G(\underline{p}, \underline{p}') \, d\Gamma_j \quad \& \quad B_j = \int_{\Gamma_j} \frac{\partial G(\underline{p}, \underline{p}')}{\partial n} \, d\Gamma_j,$$

and let us take G to be the fundamental solution in two-dimensional space. Then we begin by deriving the integral to $A_j(\underline{p})$. Consider $\underline{p} \notin \Gamma_j$ (i.e. $\underline{p}$ not on the boundary element, so $ab \neq 0$ in Figure 2.4 below).

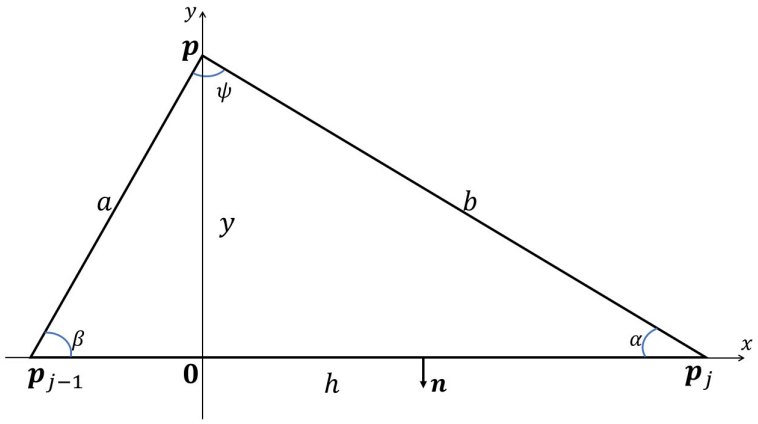

Figure 2.4: Triangle created by $\underline{p} \in \Omega$ and the endpoints $\underline{p}_j$ & $\underline{p}_{j-1}$ of an arbitrary boundary element Γ_j.

Let H_A & H_B denote the displacement from the origin to $\underline{p}_{j-1}$ & $\underline{p}_j$ respectively, such that $H_A = -a\cos(\beta)$ and $H_B = b\cos(\alpha)$. So

$$A_j(\underline{p}) = \int_{\Gamma_j} G(\underline{p}, \underline{p}')\, d\Gamma_j(\underline{p}') = -\frac{1}{2\pi}\int_{H_A}^{H_B} \ln\left((x^2+y^2)^{\frac{1}{2}}\right) dx$$

$$= -\frac{1}{2\pi}\left[x\ln\left((x^2+y^2)^{\frac{1}{2}}\right)\right]_{H_A}^{H_B} + \frac{1}{2\pi}\int_{H_A}^{H_B} \frac{x^2}{x^2+y^2}\, dx.$$

But $\frac{x^2}{x^2+y^2} = \frac{x^2+y^2-y^2}{x^2+y^2} = 1 - \frac{y^2}{x^2+y^2}$ and $\frac{d}{dx}\left(\arctan\left(\frac{x}{a}\right)\right) = \frac{a}{a^2+x^2}$, so

$$A_j(\underline{p}) = -\frac{1}{2\pi}\left[x\ln\left((x^2+y^2)^{\frac{1}{2}}\right)\right]_{H_A}^{H_B} + \frac{1}{2\pi}\left[x - y\arctan\left(\frac{x}{y}\right)\right]_{H_A}^{H_B}$$

$$= -\frac{1}{2\pi}\left[H_B\ln\left((H_B^2+y^2)^{\frac{1}{2}}\right) - H_A\ln\left((H_A^2+y^2)^{\frac{1}{2}}\right) - (H_B - H_A) + y\arctan\left(\frac{H_B}{H_A}\right)\right].$$

But $H_A = -a\cos(\beta)$, $h = H_B - H_A$, and $\psi = \arctan\left(\frac{H_B}{H_A}\right)$. From Figure 2.4 above, we can use basic trigonometry to show that $(H_A^2 + y^2)^{\frac{1}{2}} = a$, $(H_B^2 + y^2)^{\frac{1}{2}} = b$, and $y = a\sin(\beta)$. So

$$A_j(\underline{p}) = -\frac{1}{2\pi}\left[(h + H_A)\ln(b) - H_A\ln(a) - h + y\psi\right]$$

$$= -\frac{1}{2\pi}\left[h\ln(b) - a\cos(\beta)\ln(b) + a\cos\beta\ln(a) - h + a\psi\sin(\beta)\right]$$

$$= -\frac{1}{2\pi}\left[a\cos(\beta)\ln\left(\frac{a}{b}\right) - h(1-\ln(b)) + a\psi\sin(\beta)\right].$$

Now consider $\underline{p} \in \Gamma_j$ (i.e. $\underline{p}$ on the boundary element, so $ab = 0$ in Figure 2.4). We must now solve

$$A_j(\underline{p}) = -\frac{1}{2\pi}\int_0^h \ln x\, dx = -\frac{1}{2\pi}h(\ln(h) - 1).$$

Thus

$$A_j(\underline{p}) = -\frac{1}{2\pi}\begin{cases} h(\ln(h)-1), & \text{if } ab = 0. \\ a\cos(\beta)\ln\left(\frac{a}{b}\right) - h(1-\ln(b)) + a\psi\sin(\beta), & \text{if } ab \neq 0. \end{cases} \tag{2.8}$$

Now we turn to the integral given by $B_j(\underline{p})$. Consider again $\underline{p} \notin \Gamma_j$ (i.e. $ab \neq 0$), so

$$B_j(\underline{p}) = -\frac{1}{2\pi}\int_{\Gamma_j} \frac{\partial \ln|\underline{p} - \underline{p}'|}{\partial n_{\underline{p}'}}\, d\Gamma_j(\underline{p}')$$

$$= -\frac{1}{2\pi}\int_{H_A}^{H_B} \frac{\partial \ln\left((x^2+y^2)^{\frac{1}{2}}\right)}{\partial y}\, dx = -\frac{1}{2\pi}\int_{H_A}^{H_B} \frac{y}{x^2+y^2}\, dx$$

$$= -\frac{1}{2\pi}\left[\arctan\left(\frac{x}{y}\right)\right]_{H_A}^{H_B} = -\frac{1}{2\pi}\arctan\left(\frac{H_B}{H_A}\right) = -\frac{1}{2\pi}\psi.$$

For $\underline{p} \in \Gamma_j$ (i.e. $ab = 0$),

$$B_j(\underline{p}) = -\frac{1}{2\pi}\int_{\Gamma_j} \frac{\partial \ln x}{\partial y}\, d\Gamma_j(\underline{p}') = 0.$$

Thus, if Ω is convex,

$$B_j(\underline{p}) = -\frac{1}{2\pi}\begin{cases} 0, & \text{if } ab = 0. \\ \psi, & \text{if } ab \neq 0. \end{cases} \tag{2.9}$$

So now, for $\underline{p} \in \Omega$, equation (2.7) can be given by

$$T(\underline{p}) = \sum_{j=1}^{N} T_j' A_j(\underline{p}) - \sum_{j=1}^{N} T_j B_j(\underline{p}) \tag{2.10}$$

We then apply equation (2.10) at the nodes $\underline{\tilde{p}}_i$ for $i = 1, \ldots, N$ to obtain a system of N linear algebraic equations

$$\sum_{j=1}^{N}[A_{ij}T_j' + B_{ij}T_j] = 0 \tag{2.11}$$

where matrices A and B are given by $A_{ij} = A_j(\underline{\tilde{p}}_i)$ and $B_{ij} = -B_j(\underline{\tilde{p}}_i) - \delta_{ij}/2$ for $i, j = 1, \ldots, N$. Finally we impose the boundary conditions

$$cT_i + dT_i' = f(\underline{\tilde{p}}_i) \tag{2.12}$$

for $i = 1, \ldots, N$ to obtain another system of N equations, forming overall with equation (2.11) a system of $2N$ linear algebraic equations. In Chapter 4, we will see explicitly how to manipulate these equations for Dirichlet and Robin boundary conditions in order to solve concrete examples numerically.

Chapter 3

Boundary Element Method for other Partial Differential Equations

We have seen how the BEM is implemented for Laplace's equation, but now we are interested in solving problems with different PDEs inside the boundary. One mathematical tool we may use here is a transformation of the PDE inside the domain, so that this PDE takes the form of something that can be formulated into a boundary integral equation. Note that in this case, the boundary conditions must also be reformulated under the transformation. Alternatively, one may use Green's identities to change the PDE from a domain problem to a boundary problem in integral form.

3.1 Steady-State Heat Equation

The steady-state heat equation is determined by $\nabla \cdot (k(\underline{x})\nabla T(\underline{x})) = 0$ with $k(\underline{x}) > 0$. If $\nabla^2 f = 0$, where $f = k^{\frac{1}{2}}$, using the transformation $u = fT$, we can recast the heat equation into the Laplace equation. We begin by inserting $f^2 = k$ into the heat equation and expanding using both the product and chain rules, so

$$\nabla \cdot (k(\underline{x})\nabla T(\underline{x})) = \nabla \cdot (f^2(\underline{x})\nabla T(\underline{x})) = f^2 \nabla \cdot \nabla T + \nabla T \cdot \nabla f^2$$

$$= f^2 \nabla^2 T + \nabla T \cdot (2f \nabla f) = 0.$$

But $f > 0$ since $k(\underline{x}) > 0$, so

$$f\nabla^2 T + 2\nabla f \cdot \nabla T = 0.$$

We have assumed that $\nabla^2 f = 0$, so we can add the zero term $T\nabla^2 f$ to the equation to get

$$0 = f\nabla^2 T + 2\nabla f \cdot \nabla T + T\nabla^2 f = \nabla^2 fT = \nabla^2 u.$$

Thus we have shown that $\nabla \cdot (k(\underline{x})\nabla T(\underline{x})) = 0$ is recast as $\nabla^2 u = 0$ with the transformation $u = fT$. We can also determine how the boundary conditions are affected under the transformation.

i) *Dirichlet boundary condition*: $T = \overline{T}$ on $\partial\Omega$. So $fT = f\overline{T}$ on $\partial\Omega$, but we are using the transformation $u = fT$, so

$$u = f\overline{T} \quad \text{on } \partial\Omega.$$

ii) *Neumann boundary condition*: $k\frac{\partial T}{\partial n} = \overline{T}'$ on $\partial\Omega$. Using $k = f^2$ & $T = \frac{u}{f}$ (noting that $f(\underline{x}) \neq 0 \quad \forall\, \underline{x} \in \Omega$), we get

$$k\frac{\partial T}{\partial n} = f^2 \frac{\partial}{\partial n}\left(\frac{u}{f}\right) = f^2 \nabla\left(\frac{u}{f}\right) \cdot n$$

$$= f^2\left(\frac{f\nabla u - u\nabla f}{f^2}\right) \cdot n = (f\nabla u - u\nabla f) \cdot n = f\frac{\partial u}{\partial n} - u\frac{\partial f}{\partial n},$$

so we have shown that

$$f\frac{\partial u}{\partial n} - u\frac{\partial f}{\partial n} = \overline{T}' \quad \text{on } \partial\Omega.$$

3.2 Nonlinear Heat Equation

The nonlinear heat equation, given by $\nabla \cdot (k(T)\nabla T(\underline{x})) = 0$ with $k > 0$ can be formed into the Laplace equation $\nabla^2\psi = 0$ using the Kirchhoff transformation $\psi = \int_0^T k(\tau)\, d\tau$ (see Khader & Hanna, 1981, cited in Ingham & Kelmanson, 1984, p.9). To show this, we follow the rationale set by Brebbia *et al* (1984, p.103) and define the variable $\psi(T)$ such that

$$\nabla\psi = \frac{d\psi}{dT}\nabla T. \tag{3.1}$$

Looking at the right hand side of equation (3.1) and comparing to the heat equation $\nabla \cdot (k(T)\nabla T(\underline{x})) = 0$, we now define ψ so that

$$\frac{d\psi}{dT} = k(T), \tag{3.2}$$

which gives

$$\psi = \int_0^T k(\tau)\, d\tau.$$

Putting (3.2) into (3.1), we see

$$\nabla\psi = k(T)\nabla T(\underline{x}). \tag{3.3}$$

Taking the divergence of both sides of (3.3) gives

$$\nabla^2\psi = \nabla\cdot(k(T)\nabla T(\underline{x})) = 0.$$

Therefore, the Kirchhoff transformation $\psi = \int_0^T k(\tau)\,d\tau$ recasts $\nabla\cdot(k(T)\nabla T(\underline{x})) = 0$ as the Laplace equation $\nabla^2\psi = 0$. We can also determine how the boundary conditions are affected under the transformation.

i) *Dirichlet boundary condition*: $T = \overline{T}$ on $\partial\Omega$. So then on the boundary $\partial\Omega$, it must also be true that $\psi(T) = \psi(\overline{T})$. Thus, using the definition of ψ, we have shown

$$\psi = \int_0^{\overline{T}} k(\tau)\,d\tau \quad \text{on } \partial\Omega.$$

ii) *Neumann boundary condition*: $k\frac{\partial T}{\partial n} = \overline{T}'$ on $\partial\Omega$. We can write this as $(k\nabla T)\cdot\underline{n} = \overline{T}'$, but equation (3.3) shows $k\nabla T = \nabla\psi$.

Thus $\nabla\psi\cdot\underline{n} = \overline{T}'$, which is equivalent to

$$\frac{\partial\psi}{\partial n} = \overline{T}' \quad \text{on } \partial\Omega.$$

3.3 Biharmonic Equation

The biharmonic equation is given by $\nabla^4\psi = \nabla^2(\nabla^2\psi) = 0$ and can model the slow flow of viscous fluids. For this equation, we can define ω such that $\nabla^2\psi = \omega$ and $\nabla^2\omega = 0$. Then ω satisfies Laplace's equation, so can take the form $\eta\omega = \int_{\partial\Omega}\left[G\frac{\partial\omega}{\partial n} - \omega\frac{\partial G}{\partial n}\right]dS$ using Green's identity. But ψ is in the form of Poisson's equation, which can take the form of

$$\eta\psi = \int_{\partial\Omega}\left[G\frac{\partial\psi}{\partial n} - \psi\frac{\partial G}{\partial n}\right]dS - \int_\Omega G\omega\,d\Omega. \tag{3.4}$$

We now want to turn the second integral in equation (3.4) from a domain integral (integrating over Ω) into a boundary integral (integrating over $\partial\Omega$). To do that, we define a function $E(\underline{p},\underline{p}') = \frac{r^2}{8\pi}[\ln(r) - 1]$ such that $\nabla^2 E = -G$. Then we must employ Green's identity by noticing the harmonic property of ω (i.e. $\nabla^2\omega = 0$). More precisely, we observe

$$-\int_\Omega G\omega\,d\Omega = \int_\Omega \omega\nabla^2 E\,d\Omega = \int_{\partial\Omega}\left[\omega\frac{\partial E}{\partial n} - E\frac{\partial\omega}{\partial n}\right]dS. \tag{3.5}$$

To obtain an equation operating only on the boundary, we simply insert (3.5) back into (3.4) to find our new boundary integral equation solving the biharmonic equation $\nabla^4\psi = 0$

$$\eta\psi = \int_{\partial\Omega}\left[G\frac{\partial\psi}{\partial n} - \psi\frac{\partial G}{\partial n}\right]dS + \int_{\partial\Omega}\left[\omega\frac{\partial E}{\partial n} - E\frac{\partial\omega}{\partial n}\right]dS. \tag{3.6}$$

Chapter 4

Examples using Computational Numerical Methods

This chapter will apply the theory of the previous chapters to specific problems that show in more detail how the boundary element method operates and under which conditions it works best. We will look at different boundary conditions to see how the method deals with these, but firstly we will look at two types of errors which will allow us to evaluate how well our numerical methods have worked. Suppose we are finding an approximation x_N to the exact value x^*. Then the

- **absolute error** is given by
$$|x^* - x_N|,$$
i.e. the difference between the exact value and our approximation.
- **relative error** is given by
$$\left|\frac{x^* - x_N}{x^*}\right|,$$
i.e. the magnitude of the absolute error relative to the exact value x^*.

4.1 Dirichlet Boundary Condition

Let $\Omega = \{(x, y) \mid x^2 + y^2 < 1\}$ be the unit circle and let $T(x, y) = xy$ be the solution of the Dirichlet problem

$$\begin{cases} \nabla^2 T(x, y) = 0 & \text{for } (x, y) \in \Omega, \\ T(x, y) = xy & \text{for } (x, y) \in \partial\Omega. \end{cases}$$

We will solve this using the BEM in python to obtain numerical results and compare these to analytical (exact) solutions to see how the BEM works in a basic example. From

equations (2.11) and (2.12), we now have the following system of $2N$ equations for the Dirichlet problem:

$$\begin{cases} A\underline{u}' + B\underline{u} = \underline{0} & (N \text{ Equations}), \\ \underline{u} = \underline{f} & (N \text{ Equations}), \end{cases}$$

for $A, B \in \mathbb{R}^{N\times N}$, and so we have been given $\underline{u}$ as part of the Dirichlet boundary condition. In order to solve this system of equations, we can now substitute $\underline{f}$ to get $A\underline{u}' + B\underline{f} = \underline{0}$ such that we are now only tasked with solving a system of N equations, as we have eliminated N equations from the boundary condition via the substitution. To solve for $\underline{u}'$, we can simply rearrange this equation and solve $\underline{u}' = -A^{-1}B\underline{f}$ (see Appendix A.1).

	$T(0.5, 0.5)$	Abs. Error
$N = 20$	0.246684	0.003315
$N = 40$	0.249193	0.000807
$N = 80$	0.249803	0.000197
Exact	0.250000	-

Table 4.1: Numerically determined solutions to the Dirichlet boundary condition problem.

As one would expect, as the number of boundary elements N increases, so does the accuracy of the numerical solutions. This is due to the fact that more (smaller) elements can better replicate the curvature of the circle. Thus as N increases, the numerical solution converges to the analytical solution (given by $T(x, y) = xy$, so $T(0.5, 0.5) = 0.25$), as seen in Table 4.1 and graphically in Figure B.1 (see Appendix B).

4.2 Robin Boundary Condition

Let $\Omega = \{(x, y) \mid x^2 + y^2 < 4\}$ be the disk of radius 2 and let T be the solution of the Laplace equation

$$\nabla^2 T(x, y) = 0 \qquad (x, y) \in \Omega$$

subject to the Robin boundary condition

$$T(x, y) + \frac{\partial T}{\partial n}(x, y) = x \qquad (x, y) \in \partial\Omega$$

where $\partial\Omega = \{(x, y) \mid x^2 + y^2 = 4\}$ is the boundary of Ω and $\mathbf{n}$ is the outward unit normal to the boundary.

Once again from equations (2.11) and (2.12), we now have the following system of $2N$ equations for the Robin boundary condition problem:

$$\begin{cases} A\underline{u}' + B\underline{u} = \underline{0} & (N \text{ Equations}), \\ \underline{u} + \underline{u}' = \underline{g} & (N \text{ Equations}), \end{cases} \tag{4.1}$$

and so now we have not been given $\underline{u}$ or $\underline{u}'$ directly, so we cannot proceed like before with substitution. Instead, we must use elimination, whereby we write $\underline{u}'$ in terms of $\underline{u}$ (or $\underline{u}$ in terms of $\underline{u}'$) in order to eliminate one term from the system of equations. So we can rearrange the boundary condition to get $\underline{u}' = \underline{g} - \underline{u}$. Then, putting this into the first system, we get $A(\underline{g} - \underline{u}) + B\underline{u} = \underline{0}$ which is equivalent to $(A - B)\underline{u} = A\underline{g}$ and from here we simply solve $\underline{u} = (A - B)^{-1}A\underline{g}$ (see Appendix A.2).

	$(0.2, 0.2)$	$(1.0, 0.2)$	$(1.8, 0.2)$
$N = 8$	0.127388	0.636973	1.134828
$N = 16$	0.131895	0.659472	1.188592
$N = 32$	0.132676	0.664881	1.196696
$N = 64$	0.133244	0.666221	1.199202
Exact	0.133333	0.666666	1.200000

Table 4.2: Numerically determined solutions to the Robin boundary condition problem.

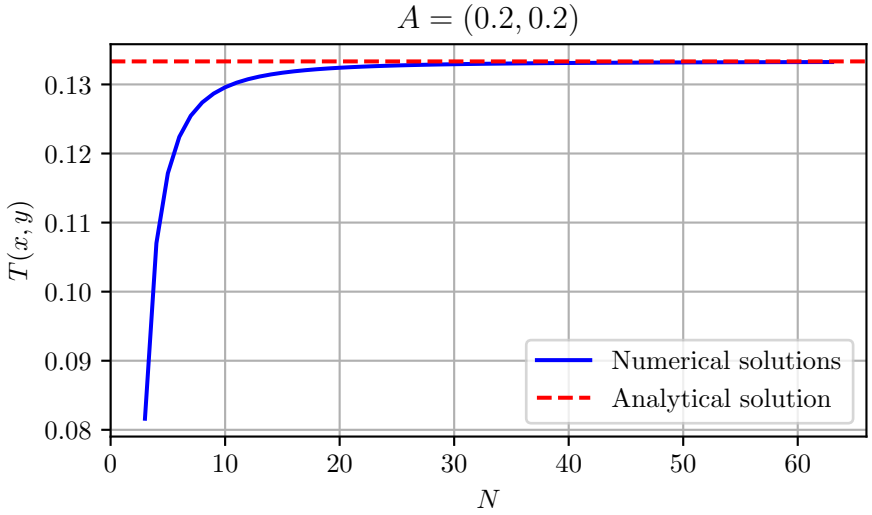

Figure 4.1: Numerically determined solutions at the point $A = (0.2, 0.2)$ to the Robin boundary condition problem as N increases.

We will now use the BEM to determine the numerical solutions at the points $A = (0.2, 0.2)$, $B = (1.0, 0.2)$, and $C = (1.8, 0.2)$ for $N \in \{8, 16, 32, 64\}$ boundary elements.

As before, as the number of boundary elements N increases, the numerical solutions converge to the analytical solutions (given by $T(x, y) = 2x/3$), as seen in Table 4.2. Furthermore, this behaviour is clearly demonstrated in Figure 4.1, where the numerical solutions at each of the points seem to become accurate approximations to the analytical solutions quickly, namely for around $N \geq 25$. See also Appendix B for Figures B.2 and B.3 demonstrating the same behaviour for $B = (1.0, 0.2)$ and $C = (1.8, 0.2)$ respectively.

4.2.1 Errors of the Numerical Solutions

To examine the accuracy of the numerical solutions in finer detail, we must first consider the absolute errors.

	$(0.2, 0.2)$	$(1.0, 0.2)$	$(1.8, 0.2)$
$N = 8$	0.005946	0.029693	0.065172
$N = 16$	0.001439	0.007195	0.011408
$N = 32$	0.000357	0.001786	0.003304
$N = 64$	0.000089	0.000446	0.000798

Table 4.3: Absolute errors to the numerically determined values in Table 4.2.

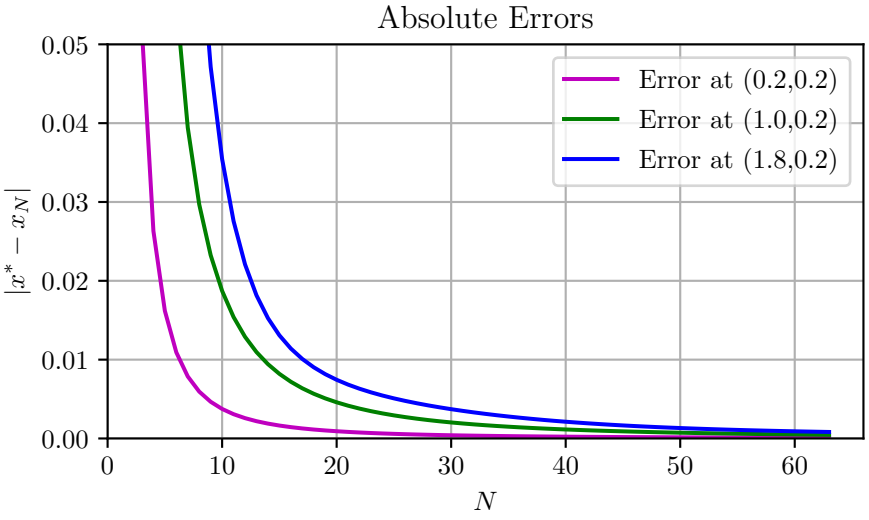

Figure 4.2: Absolute errors to the numerically determined values in Table 4.2 as N increases.

We have determined the absolute errors by using the exact solution $T(x, y) = 2x/3$. As can be seen clearly from Table 4.3, the absolute error is decreasing as N increases and this is consolidated in Figure 4.2. However, there seems to be a noticeable difference between the errors of the varying points, namely it appears that the approximation to the point

$A = (0.2, 0.2)$ is closer to the analytical solution than the other approximations are to their respective exact values. This gap closes as N increases, but the data from Table 4.3 shows a clear difference in the accuracy. For example, take $N = 64$ and compare the absolute error 0.000089 at the point $(0.2, 0.2)$ with 0.000798 at $(1.8, 0.2)$. What we must now determine is whether this disparity is due to the fact that the BEM is less accurate closer to the boundary, or if it proportional to the increase in the value of the point that we are estimating. To check this, we proceed with the relative errors.

	$(0.2, 0.2)$	$(1.0, 0.2)$	$(1.8, 0.2)$
$N = 8$	0.044591	0.044540	0.054310
$N = 16$	0.010791	0.010792	0.009507
$N = 32$	0.002679	0.002679	0.002753
$N = 64$	0.000669	0.000669	0.000665

Table 4.4: Relative errors to the numerically determined values in Table 4.2.

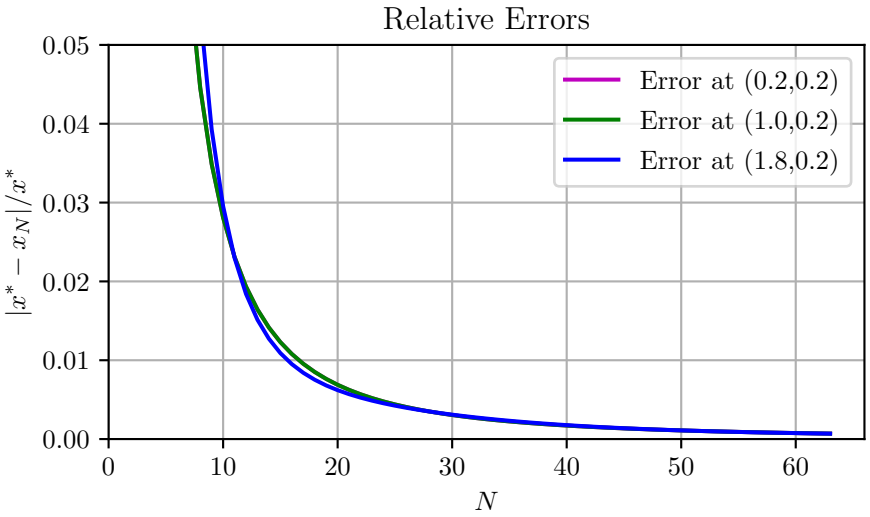

Figure 4.3: Relative errors to the numerically determined values in Table 4.2 as N increases.

The magnitudes of the relative errors at each of the three points are remarkably close for all values of N. They are so close in fact that the errors at the point $(0.2, 0.2)$ are indistinguishable from those at $(1.0, 0.2)$ in Figure 4.3. Table 4.4 shows just how close the relative errors are, and some are even identical to 6 decimal places. The conclusion we can draw from this data is that the BEM is equally as effective in the middle of the domain as it is closer to the boundary, and that the varying absolute errors occurred only because the inputted values were of different sizes, and so the errors changed proportionally to the size of the input.

4.2.2 Order of Convergence

By comparing the absolute errors in Table 4.3, it can be seen that as the number of elements N doubles, the absolute error reduces by a factor of 4 (i.e. the numerical solution becomes 4 times more accurate), which implies that the solution converges *quadratically* (order 2) as N increases. Kirkup & Henwood (1994) observe that the absolute errors $\varepsilon \propto N^{-\alpha}$ where α is the rate of convergence (p.35). So let $\varepsilon_1 = AN_1^{-\alpha}$ and $\varepsilon_2 = AN_2^{-\alpha}$ for some constant A. Then $\varepsilon_1/\varepsilon_2 = N_1^{-\alpha}/N_2^{-\alpha}$ and so the rate of convergence α can be approximated by

$$\alpha \approx -\frac{\log\left(\varepsilon_1/\varepsilon_2\right)}{\log\left(N_1/N_2\right)}. \tag{4.2}$$

As one of many possible examples, consider $N_1 = 32$ and $N_2 = 64$ at the point $A = (0.2, 0.2)$ from Table 4.3. Then, using equation (4.2) with the corresponding absolute errors $\varepsilon_1 = 0.000357$, $\varepsilon_2 = 0.000089$, we find that $\alpha \approx 2.004$. Thus the convergence of the method to the exact solution is indeed quadratic. Similar findings can be shown for an unlimited number of elements, but including this would be cumbersome and unnecessary, and so here the reader is invited to calculate α with different values from Table 4.3 or otherwise if they are worried about casuistic data. The same order of convergence can be shown for the Dirichlet problem in Section 4.1 by also observing the same change in absolute errors seen in Table 4.1.

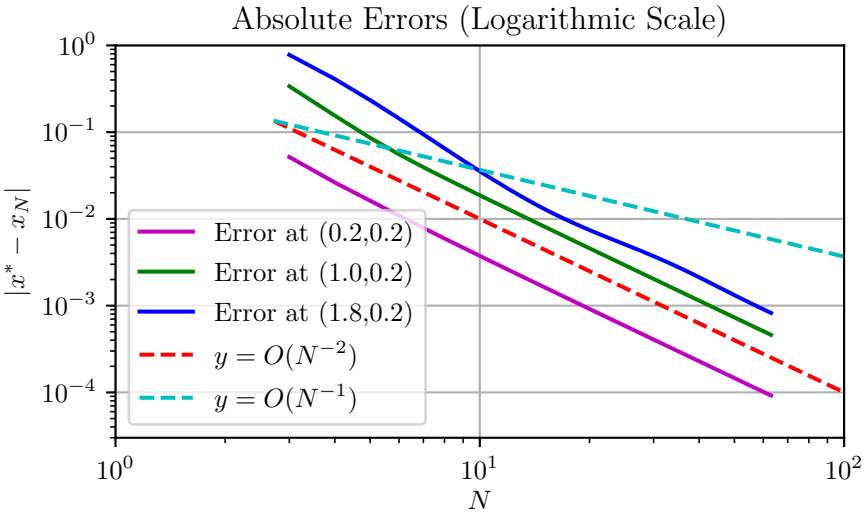

Figure 4.4: Logarithmic scale of the absolute errors shown in Figure 4.2 compared with linear and quadratic convergence.

Furthermore, we can look at the gradients of the absolute errors on a logarithmic scale to evaluate how they approach 0. From Figure 4.4, we can see that the errors approach 0 parallel to N^{-2} and are clearly not parallel to N^{-1}. Therefore, we can see graphically that

the method is converging to the exact solution with order 2. As before, this behaviour can also be shown to be true for the Dirichlet problem in Section 4.1.

4.2.3 Evaluating the Normal Derivative

Finally, from the Robin type problem, it is possible to determine numerical solutions to the normal derivative given by $\frac{\partial T}{\partial n}(x, y)$, and we may also compare them to the exact solutions. The normal derivative will be evaluated over 8 boundary elements as seen in Figure 4.5.

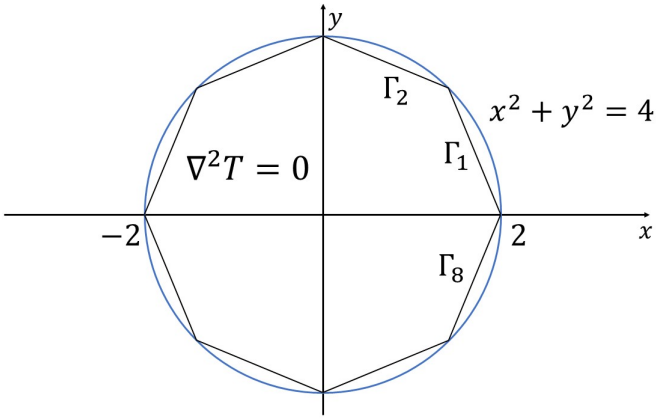

Figure 4.5: Boundary $\partial\Omega = \{(x, y) \mid x^2 + y^2 = 4\}$ discretised into 8 boundary elements

Firstly, to find the exact solutions, we use the analytical solution for T on the boundary with polar coordinates as such

$$T(x, y) = \frac{2x}{3} = \frac{2r\cos\theta}{3}.$$

Then we can see

$$\frac{\partial T}{\partial r} = \frac{2\cos\theta}{3} = \frac{2r\cos\theta}{3r} = \frac{2x}{3r} = \frac{x}{3}$$

when evaluated at $r = 2$. To determine the value of x_i on the circle corresponding to boundary element Γ_i (see Figure 4.5), we use $x_i = 2\cos((2i-1)\pi/8)$ for $i = 1, \ldots, 8$. Then for the exact solutions we solve $x_i/3$. For the numerical solutions, we return to equation (4.1) and rearrange the boundary condition in the code to get $\underline{u}' = \underline{g} - \underline{u}$ where $\underline{g}$ is the x-coordinate of the midpoint of each boundary element and $\underline{u}$ has been numerically determined using the BEM.

Now from Table 4.5 we can see the numerical approximations of $\frac{\partial T}{\partial n}$ when $N = 8$. As one might expect, there is a lot of symmetry in the results due to the nature of cosine (i.e. $\cos x = \cos(-x)$ and $\cos(\pi - x) = -\cos x$). We can see from the data that the numerical

Element	Numerical	Exact	Abs. Error	Rel. Error
Γ_1	0.618960	0.615920	0.003040	0.004936
Γ_2	0.256382	0.255122	0.001259	0.004936
Γ_3	-0.256382	-0.255122	0.001259	0.004936
Γ_4	-0.618960	-0.615920	0.003040	0.004936
Γ_5	-0.618960	-0.615920	0.003040	0.004936
Γ_6	-0.256382	-0.255122	0.001259	0.004936
Γ_7	0.256382	0.255122	0.001259	0.004936
Γ_8	0.618960	0.615920	0.003040	0.004936

Table 4.5: Numerically and analytically determined solutions at Γ_i to the normal derivative $\frac{\partial T}{\partial n}$ for $N = 8$ in the above Robin type problem.

approximations are accurate to around 2 decimal places. Here it is worth noting that for $N = 8$, our approximations for $T(x, y)$ in Table 4.2 were the least accurate, as shown by the absolute errors in Table 4.3, and so this small N may also affect the accuracy of these numerical results for the normal derivative. Although again it appears from the absolute errors that there is a disparity of the accuracy at certain points, the relative error shows that this only occurs because of the magnitude of the values, and in fact all of the relative errors are identical to 6 decimal places.

Conclusion

We have derived and implemented the boundary element method for the Laplace equation and have demonstrated that the method works effectively for N sufficiently large. Moreover, it has been shown that the method is equally effective on all points inside the domain and the numerical solution converges quadratically to the exact solution in the worked examples. Further work may consider boundaries of different shapes and analyse their rate of convergence, particularly for straight edges that would require fewer boundary elements to model effectively. One may also consider the rate of convergence when using nonlinear (e.g. quadratically curved) boundary elements to see how an improved model of the boundary would increase the accuracy of the results. Alongside this, an analysis of the implementation of the method using different boundary function approximations (e.g. at the endpoints) could be compared to the aforementioned source of errors in order to determine which of the two sources of errors is dominant under certain conditions. From this research, it could become clear how to reduce the magnitude of the errors and how to increase the order of convergence, thus making the method even more reliable and effective.

Bibliography

[1] Aliabadi, M.H. 2002. *Applications in Solids and Structures.* The Boundary Element Method, Vol 2. New York: Wiley.

[2] Brebbia, C. A. & Walker, S. 1980. *Boundary Element Techniques in Engineering.* London: Newnes-Butterworths.

[3] Brebbia, C.A., Telles, J.C.F., & Wrobel, L.C. 1984. *Boundary Element Techniques: Theory and Application in Engineering.* Berlin: Springer-Verlag.

[4] Brebbia, C.A. 2017. The birth of the boundary element method from conception to application. *Engineering Analysis with Boundary Elements*, **77**, pp.iii–x.

[5] Cheng, A.H.-D. & Cheng, D.T. 2005. Heritage and Early History of the Boundary Element Method. *Engineering Analysis with Boundary Elements*, **29**(3), pp.268–302.

[6] Costabel, M. 1987. Principles of Boundary Element Methods, *Computer Physics Reports.* **6**, pp.243–274.

[7] Ingham, D.B. & Kelmanson, M.A. 1984. *Boundary Integral Equation Analysis of Singular, Potential and Biharmonic Problems.* Berlin: Springer-Verlag.

[8] Kirkup, S.M. & Henwood, D.J. 1994. An Empirical Error Analysis of the Boundary Element Method Applied to Laplace's Equation. *Applied Mathematical Modelling.* **18**(1), pp. 32–38.

[9] Kythe, P.K. 1996. *Fundamental Solutions for Differential Operators and Applications*. Boston: Birkhäuser.

[10] Maor, E. 1987. *To Infinity and Beyond: a Cultural History of the Infinite.* Boston: Birkhäuser.

[11] Partridge, P.W., Brebbia, C.A., & Wrobel, L.C. 1991. *The Dual Reciprocity Boundary Element Method*. Southampton: Computational Mechanics.

[12] Sharp, B. 2021. The Fundamental Solution of the Laplacian. MATH3414 Analytical Solutions of Partial Differential Equations. 9 November, University of Leeds.

[13] Yu, K.H., Kadarman, A.H., & Djojodihardjo, H. 2010. Development and Implementation of some BEM Variants - A Critical Review. *Engineering Analysis with Boundary Elements*. **34**(10), pp.884–899.

Appendix A

Python Code

A.1 Dirichlet Boundary Condition

The following Python code solves the Dirichlet boundary condition problem on the unit disk $\Omega = \{(x, y) \mid x^2 + y^2 < 1\}$ where

$$\begin{cases} \nabla^2 T(x, y) = 0 & \text{for } (x, y) \in \Omega, \\ T(x, y) = xy & \text{for } (x, y) \in \partial\Omega \end{cases}$$

using the boundary element method.

```
import math
import numpy as np

def SOL(x,y):
    return x*y

pi=4*math.atan(1)

def DAC(x):
    if x>=1:
        DAC=0
    elif x<=-1:
        DAC=pi
    else:
        DAC=math.acos(x)
    return DAC

def res(x0,y0,N):
    x,y=[],[]
    U,DU,BU=[],[],[]
    z1,z2=[],[]
    A=np.zeros((N, N))
```

```
    B=np.zeros((N, N))
    for i in range (1,N+1):
        theta=2*pi*i/N
        x.append(math.cos(theta))
        y.append(math.sin(theta))

    for i in range (0,N):
        z1.append((x[i-1]+x[i])/2)
        z2.append((y[i-1]+y[i])/2)

    for i in range (0,N):
        for j in range (0,N):
            H=math.sqrt((x[j-1]-x[j])**2+(y[j-1]-y[j])**2)
            A0=math.sqrt((x[j-1]-z1[i])**2+(y[j-1]-z2[i])**2)
            B0=math.sqrt((x[j]-z1[i])**2+(y[j]-z2[i])**2)
            cB=(A0*A0+H*H-B0*B0)/(2*H*A0)
            sB=math.sin(DAC(cB))
            cZ=(A0*A0+B0*B0-H*H)/(2*A0*B0)
            psi=DAC(cZ)
            if i==j:
                B[i][j]=-0.5
                A[i][j]=(H-H*math.log(H/2))/(2*pi)
            else:
                B[i][j]=psi/(2*pi)
                A[i][j]=(-A0*cB*math.log(A0/B0)+H-H*math.log(B0)-A0*sB*
                                                        psi)/(2*pi)

    for i in range (0,N):
        U.append(SOL(z1[i],z2[i]))

    for i in range (0,N):
        s=0
        for j in range (0,N):
            s=s-B[i][j]*U[j]
        BU.append(s)
    DU=np.linalg.solve(A,BU)

    s=0
    for j in range (0,N):
        H=math.sqrt((x[j-1]-x[j])**2+(y[j-1]-y[j])**2)
        A0=math.sqrt((x[j-1]-x0)**2+(y[j-1]-y0)**2)
        B0=math.sqrt((x[j]-x0)**2+(y[j]-y0)**2)
        cB=(A0*A0+H*H-B0*B0)/(2*H*A0)
        sB=math.sin(DAC(cB))
        cZ=(A0*A0+B0*B0-H*H)/(2*A0*B0)
        psi=DAC(cZ)
        A=(-A0*cB*math.log(A0/B0)+H-H*math.log(B0)-A0*psi*sB)/(2.0*pi)
        B=psi/(2*pi)
        s=s+A*DU[j]+B*U[j]
```

```
    U0=s
    return U0
```

A.2 Robin Boundary Condition

The following Python code solves the Robin boundary condition problem on the circle $\Omega = \{(x, y) \mid x^2 + y^2 < 4\}$ where

$$\begin{cases} \nabla^2 T(x,y) = 0 & \text{for } (x,y) \in \Omega, \\ T(x,y) + \frac{\partial T}{\partial n}(x,y) = x & \text{for } (x,y) \in \partial\Omega \end{cases}$$

using the boundary element method.

```
import math
import numpy as np

pi=4*math.atan(1)

def DAC(x):
    if x>=1:
        DAC=0
    elif x<=-1:
        DAC=pi
    else:
        DAC=math.acos(x)
    return DAC

def res(x0,y0,N):
    x,y=[],[]
    g,Ag=[],[]
    z1,z2=[],[]
    A=np.zeros((N, N))
    B=np.zeros((N, N))
    C=np.zeros((N, N))
    for i in range (1,N+1):
        theta=2*pi*i/N
        x.append(2*math.cos(theta))
        y.append(2*math.sin(theta))

    for i in range (0,N):
        z1.append((x[i-1]+x[i])/2)
        z2.append((y[i-1]+y[i])/2)

    for i in range (0,N):
        for j in range (0,N):
            H=math.sqrt((x[j-1]-x[j])**2+(y[j-1]-y[j])**2)
```

```
            A0=math.sqrt((x[j-1]-z1[i])**2+(y[j-1]-z2[i])**2)
            B0=math.sqrt((x[j]-z1[i])**2+(y[j]-z2[i])**2)
            cB=(A0*A0+H*H-B0*B0)/(2*H*A0)
            sB=math.sin(DAC(cB))
            cZ=(A0*A0+B0*B0-H*H)/(2*A0*B0)
            psi=DAC(cZ)
            if i==j:
                B[i][j]=-0.5
                A[i][j]=(H-H*math.log(H/2))/(2*pi)
            else:
                B[i][j]=psi/(2*pi)
                A[i][j]=(-A0*cB*math.log(A0/B0)+H-H*math.log(B0)-A0*sB*
                                                        psi)/(2*pi)

    for i in range (0,N):
        g.append(z1[i])

    for i in range (0,N):
        s=0
        for j in range (0,N):
            C[i][j]=A[i][j]-B[i][j]
            s=s+A[i][j]*g[j]
        Ag.append(s)
    U=np.linalg.solve(C,Ag)

    s=0
    for j in range (0,N):
        H=math.sqrt((x[j-1]-x[j])**2+(y[j-1]-y[j])**2)
        A0=math.sqrt((x[j-1]-x0)**2+(y[j-1]-y0)**2)
        B0=math.sqrt((x[j]-x0)**2+(y[j]-y0)**2)
        cB=(A0*A0+H*H-B0*B0)/(2*H*A0)
        sB=math.sin(DAC(cB))
        cZ=(A0*A0+B0*B0-H*H)/(2*A0*B0)
        psi=DAC(cZ)
        A=(-A0*cB*math.log(A0/B0)+H-H*math.log(B0)-A0*psi*sB)/(2.0*pi)
        B=psi/(2*pi)
        s=s+A*g[j]-B*U[j]
    U0=s
    return U0
```

Appendix B

Graphs

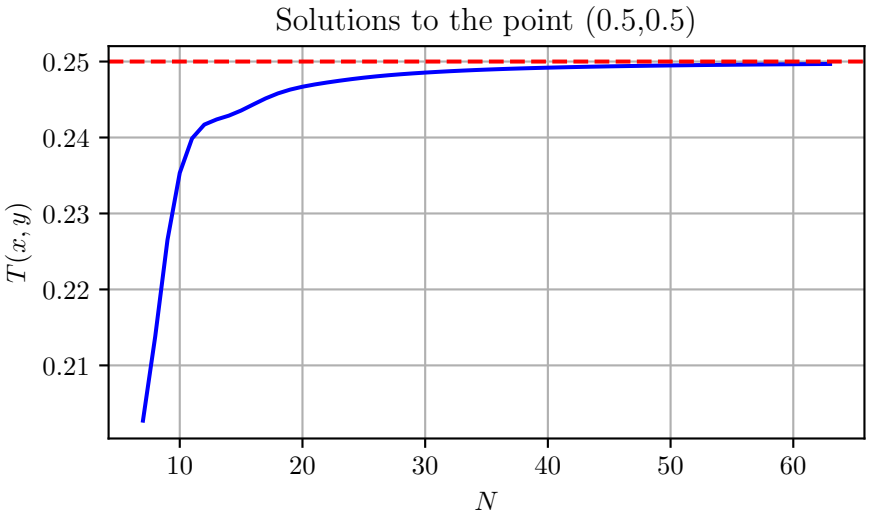

Figure B.1: Numerically determined solutions at the point $(0.5, 0.5)$ to the Dirichlet boundary condition problem in Section 4.1 as N increases.

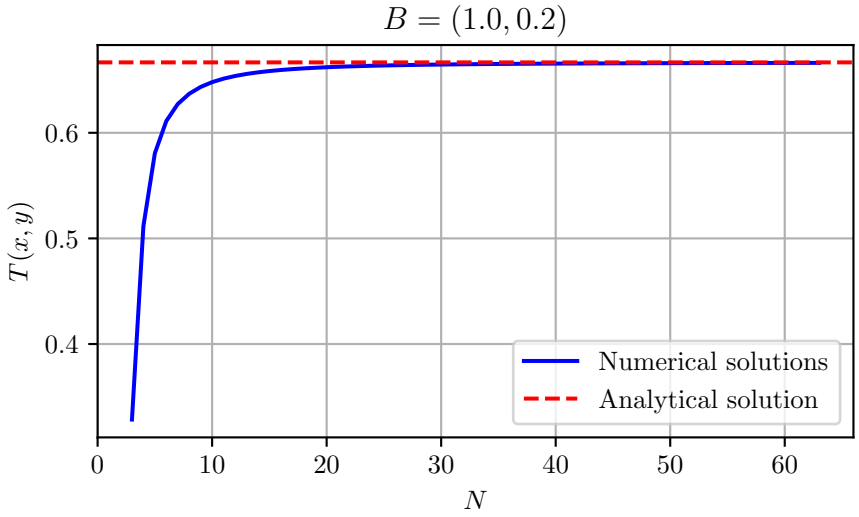

Figure B.2: Numerically determined solutions at the point $B = (1.0, 0.2)$ to the Robin boundary condition problem in Section 4.2 as N increases.

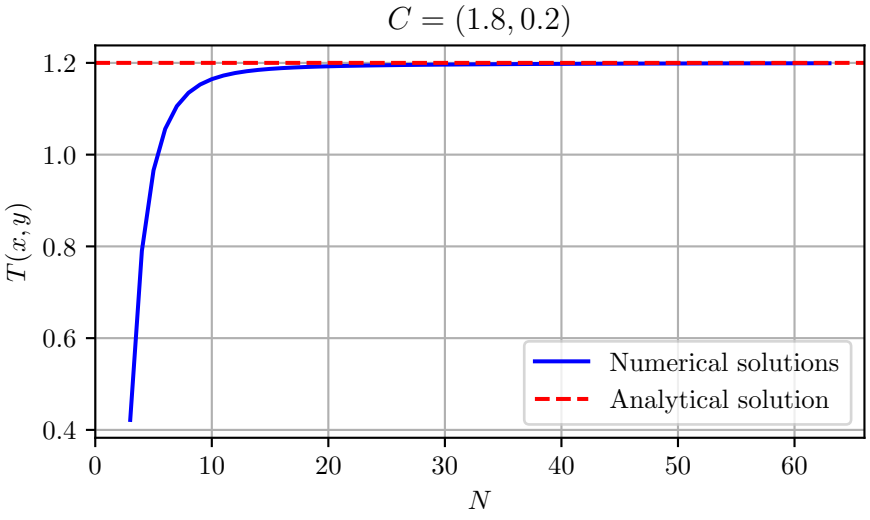

Figure B.3: Numerically determined solutions at the point $C = (1.8, 0.2)$ to the Robin boundary condition problem in Section 4.2 as N increases.